ACTA ACUSTICA UNITED WITH ACUSTICA
Vol. 93 (2007) 22 – 30

Single and Multiple Reflections in Plane Obstacle Using the Parabolic Equation Method With a Complementary Kirchhoff Approximation

François-Edern Aballéa
Ecole Polytechnique Fédérale de Lausanne (EPFL), STI ITOP LEMA, Station 11, CH-1015 Lausanne, Suisse.
francois.aballea@epfl.ch

Jérôme Defrance
Centre Scientifique et Technique du Bâtiment (CSTB), 24 rue Joseph Fourier, F-38400 Saint-Martin-d'Hères, France. j.defrance@cstb.fr

Summary
The parabolic equation (PE) is one of the numerical methods used for sound propagation simulation in complex outdoor situations. Such model is able to take several phenomena into account at the same time such as meteorology and impedances discontinuities, but it neglects backscattering. Even if this assumption is effective in many configurations, it does not allow using PE for studies of acoustic wave propagation between a source and a receiver when an obstacle (e.g. a rigid barrier, a building) is located just before the source, or just behind the receiver. In those cases, energy reflected by the obstacle is not negligible and results obtained with PE may be incorrect. This paper aims at presenting a new method able to integrate backscattering in the GFPE (Green's Function Parabolic Equation method). In this approach a complementary Kirchhoff approximation is used by setting to zero the sound pressure above the vertical obstacle. Thus, new configurations with multiple reflections can be studied. In order to point out the role played by backscattering, we first study a barrier located just behind a source. Then, a comparison with BEM (Boundary Element Method) calculations is presented in the case of a simple reflection in homogeneous and inhomogeneous atmosphere. A more complex road traffic noise configuration with two parallel barriers and meteorological effects is also studied. Results show that the complementary Kirchhoff approach seems to be promising.

PACS no. 43.28.Js

1. Introduction

Long-range acoustic waves propagation in the atmosphere is of interest for many applications, including the noise impact of road and railway infrastructures [1, 2]. For such problems, the propagation medium is often complicated, so that meteorology and terrain effects (impedances discontinuities, uneven ground) cannot be ignored [3, 4, 5]. Several numerical methods have been developed for computation of sound in an inhomogeneous atmosphere above an impedant plane: the Fast-Field Programm (FFP) [6, 7, 8], the Ray model [9, 10, 11, 12], the Gaussian Beams (GB) [13, 14, 15], the Linearized Eulerian equations (LE) [16] and the Parabolic Equation (PE) [17, 18, 19]. The parabolic equation, approximation of the Helmholtz wave equation, is one of the powerful numerical methods efficient for long-range, forward- wave propagation thought relatively general media [20, 21].

Received 21 November 2005,
accepted 27 September 2006.

Sound barriers are widely used for noise reduction near transportation infrastructures. In the presence of a vertical obstacle, the forward wave is divided into an incident wave and a reflected wave. In most of long-range sound propagation configurations the barrier is located between the source and the receiver so that only the incident diffracted wave is considered. The treatment of sound diffraction by a barrier has been intensively study in homogeneous medium [22, 23, 24, 25] and few authors have analyzed the effect of wind on barrier efficiency [26, 17, 27].

In some cases, the reflected wave has to be considered, for example when the source (or the receiver) is located between two vertical barriers. For such configurations, multiple reflections phenomenon appears whose acoustic contribution at the receiver is not negligible. The classical PE cannot be applied anymore due to the fact that it ignores backscattering and a two-way PE [28, 29] has to be used.

This paper aims at presenting a new method (call here GFPE- Kirchhoff) able to integrate backscattering in the GFPE (Green's Function Parabolic Equation) method. In this approach, the global problem (with backscattering)

is divided in several sub-problems without backscattering. The reflections on vertical obstacle are considered by using the source image method and a complementary Kirchhoff approximation.

2. The GFPE model

The GFPE was adapted for the atmospheric propagation by Gilbert [30] and Di [31] at the beginning of the 90s. This powerful method is used to describe outdoor sound propagation in inhomogeneous medium. The two dimensional calculation is initialised by an expression of the acoustic field of a monopole source on a vertical line and propagated step by step from the source to the receivers. The ground impedance and the sound speed profile may vary for each step with a low cost of calculation time. The great advantage of this method is the step of computation that may be considerably larger than the wavelength instead of a fraction of a wavelength for classical PE; the consequence is a significant decrease of computation time.

The GFPE model is based on an elliptic form of the Helmholtz equation for the harmonic sound pressure p in (r, z) coordinates,

$$\left(\frac{\partial^2}{\partial r^2} + \frac{1}{r}\frac{\partial}{\partial r} + \frac{\partial^2}{\partial z^2} + k(r,z)^2\right) p(r,z) = 0, \qquad (1)$$

with $k(r, z) = \omega/c(r, z)$ the effective wave number, $c(r, z)$ the effective sound speed and ω the angular frequency. The pressure is written

$$p(r,z) = \frac{1}{\sqrt{r}}\phi(r,z)\,\mathrm{e}^{\mathrm{j}k_r r}$$

and the azimutal derivative of the field in the wave equation is neglected. After several assumptions as far field, slow variations of the refraction index with distance and neglecting backscattering, the following one-way equation can be obtained from equation (1):

$$\frac{\partial^2\phi(r,z)}{\partial r^2} = \mathrm{j}\sqrt{Q}\,\phi(r,z), \qquad (2)$$

where the operator Q is written

$$Q = \frac{\partial^2}{\partial z^2} + k(r,z). \qquad (3)$$

For a range independent sound speed profile on a step, a solution of equation (2) is:

$$\phi(r+\Delta r, z) = \mathrm{e}^{\mathrm{j}\Delta r\sqrt{Q}}\phi(r,z). \qquad (4)$$

After many developments described by Gilbert [30] and Salomons [32], the field at $\phi(r+\Delta r, z)$ is given by

$$\phi(r+\Delta r, z) = \left[\frac{1}{2\pi}\int_{-\infty}^{+\infty}\left(\Phi(r,k') + R(k')\Phi(r-k')\right) \cdot \mathrm{e}^{\mathrm{j}\Delta r\left(\sqrt{k_r^2-k'^2}-k_r\right)}\mathrm{e}^{\mathrm{j}k'z}\,\mathrm{d}k' + 2\mathrm{j}\beta\,\Phi(r,\beta)\,\mathrm{e}^{\mathrm{j}\Delta r\left(\sqrt{k_r^2-\beta^2}-k_r\right)}\mathrm{e}^{-\mathrm{j}\beta z}\right] \cdot \mathrm{e}^{\mathrm{j}\Delta r\delta k^2(z)/(2k_r)}, \qquad (5)$$

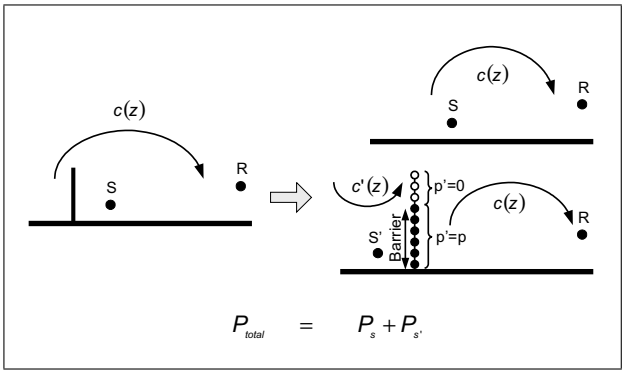

Figure 1. GFPE-Kirchhoff method applied to a barrier located behind the source. The curved rays stand for the meteorological effects. $c(z) = c'(z) = c_0$ in homogeneous atmosphere. $c(z)$ and $c'(z)$ represent respectively the downwind effect and the new profile for the propagation from the image source to the barrier.

with

$$\Phi(r,z) = \int_0^\infty \phi(r,z)\mathrm{e}^{-\mathrm{j}kz'}\,\mathrm{d}z$$

the Fourier transform of ϕ and where the wave number $k(r, z)$ is split into a reference wave number k_r at zero height and δk the small variation with height. $\beta = k_r/Z_g$ represents the surface wave pole in the reflecting coefficient $R(k')$. Equation (5) is the product of an exponential factor $\mathrm{e}^{\mathrm{j}\Delta r\delta k^2(z)/(2k_r)}$, contribution of the non-constant sound speed profile, and of 3 terms $\Phi(r, k')$, $R(k')\Phi(r, -k')$ and $\Phi(r, \beta)$ respectively representing the direct wave, the reflected wave by the ground and the surface wave. Details about the numerical implementation of equation (5) is discussed in references [32, 33].

3. The GFPE-Kirchhoff approach

The parabolic equation neglects the effects due to backward wave. Even if this assumption is correct in most of cases, numerous configurations need to be studied with backscattering. The GFPE-Kirchhoff is a way to solve this problem.

3.1. Single reflection in homogeneous medium

The method for a single reflection on a vertical obstacle located behind the source is introduced here (Figure 1). It will be extended to multiple reflections in section 3.3.

In this approach, backscattering due to sound reflection on vertical obstacles is considered by using a complementary Kirchhoff approximation [34, 35]. "Complementary" means that the principle is the same as in the case of diffraction by a straight barrier [36] (a series of receivers at the barrier calculation step has their pressure set to zero) but with the introduction of an image-source and applying a complementary Kirchhoff approximation to receiver position above the barrier.

For such configurations, two calculations have to be done. First, a "classical" GFPE calculation is performed

to evaluate the acoustic pressure at the receiver without the obstacle effect. The second calculation is achieved to determine the part of the acoustic energy reflected by the obstacle back to the receiver. For this, an image-source S' is constructed relatively to the barrier vertical plane. Its contribution is calculated with the GFPE. At the barrier step ($r = r_{\text{barrier}}$) the complementary Kirchhoff approximation is applied, i.e. the sound pressure at any calculation point above the obstacle is set to zero,

$$\left\{ \begin{array}{ll} p'(r_{\text{barrier}}, z) = p(r_{\text{barrier}}, z), & z < h_{\text{barrier}}, \\ p'(r_{\text{barrier}}, z) = 0, & z \geq h_{\text{barrier}}, \end{array} \right\} \quad (6)$$

with h_{barrier} the height of the vertical obstacle (Figure 1).

As an approximation for an absorbant barrier, the calculated fields on its surface are multiplied by the plane wave reflection coefficient $R_p = (Z_g - 1)/(Z_g + 1)$ determined from the material impedance Z_g,

$$\left\{ \begin{array}{ll} p'(r_{\text{barrier}}, z) = R_p \cdot p(r_{\text{barrier}}, z), & z < h_{\text{barrier}}, \\ p'(r_{\text{barrier}}, z) = 0, & z \geq h_{\text{barrier}}, \end{array} \right\} \quad (7)$$

and then propagated to the receiver.

At last, the total pressure p_{total} at the receiver is the sum of p_S, the direct field above ground calculation, and $p_{S'}$, the field due to the image-source S' (Figure 1).

3.2. Single reflection in inhomogeneous medium

In outdoor acoustics, variations of sound speed profiles are mainly due to temperature and wind fluctuations. In two dimensions, the sound speed profile $c(z)$ is given by

$$c(z) = c_T(z) + c_w(z), \quad (8)$$

where

$$c_T(z) = \sqrt{\frac{c_p}{c_v} R_{\text{gaz}} T_v}\,, \qquad c_w(z) = w(z). \quad (9)$$

In equation (9), c_T is the contribution of the temperature, c_p the specific heat capacity at constant pressure, c_v the specific heat capacity at constant volume, R_{gaz} the specific gaz constant in dry air and T_v the virtual temperature. c_w is the wind contribution where $\vec{v}(r, z)$ is a vector representative of the wind flow and $w(z)$ the wind component in the direction of the sound propagation.

The way to introduce meteorological effects in the GFPE-Kirchhoff depends if inhomogeneities are due to temperature gradient or to wind speed variation. These two phenomena have to be studied separately.

The wind profile can be represented by series of height dependant vectors. Its contribution depends on the propagation direction. Thus, a new sound speed profile c' has to be built for the propagation from the image source S' to the obstacle (Figure 1),

$$c'(z) = c_0 - w(z). \quad (10)$$

The temperature profile is represented by a scalar. Sound speed gradient is identical independently to propagation direction of the acoustics waves. Sound speed profile $c'(r, z)$ is written

$$c'(z) = c(z) = \sqrt{\frac{c_p}{c_v} R_{\text{gaz}} T_v}. \quad (11)$$

For a sound speed profile due to vertical temperature and wind gradients, the new speed $c'(z)$ to be used in the GFPE-Kirchhoff method is given by

$$c'(z) = c_T(z) - c_w(z) = \sqrt{\frac{c_p}{c_v} R_{\text{gaz}} T_v} - w(z). \quad (12)$$

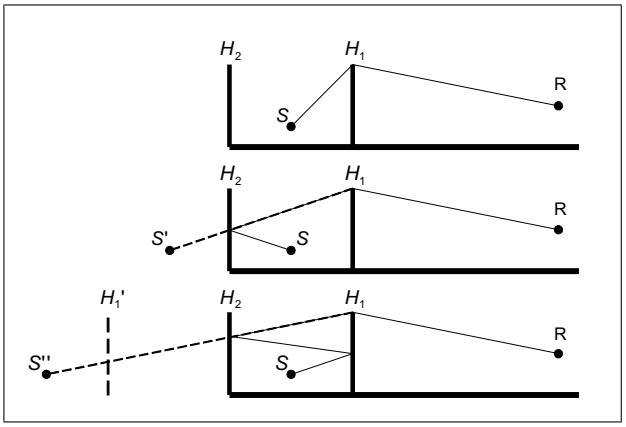

Figure 2. Different paths of propagation with two parallel barriers at the order 2 of reflection.

3.3. Multiple reflections in homogeneous medium

Backscattering due to a vertical obstacle located behind the source has been studied in homogeneous and in inhomogeneous media with the GFPE-Kirchhoff method in sections 3.1 and 3.2, respectively. In the present section, the method is extended to a source located between two parallel vertical obstacles. For such a configuration multiple reflections occur and have to be taken into account.

To introduce the multiple reflections, a set of image-sources is built for each path of propagation (Figure 2). The pressure at the receiver is the sum of each image-sources contribution. The principle of the GFPE-Kirchhoff at the order 2 (maximum of two successive reflections on obstacles) is presented Figure 3. In this case, two image-sources S' and S'' are built. Contribution of the source S is achieved by a classical GFPE calculation with one diffraction on barrier H_1 (Figure 3a). The second calculation from the image-source S' corresponds to the path with only one reflection on the obstacle. S' is constructed relatively to barrier vertical plane H_2. Its acoustic field is calculated with a complementary Kirchhoff approach at barrier H_1 and a diffraction at barrier H_2 (Figure 3b). The same principle is applied to the source S'', image of S relatively to the obstacle H_1' (symmetrical to H_1). S'' represents the acoustic path with two reflections on obstacles and one diffraction. Its contribution to the pressure at the receiver is obtained after the use of two complementary Kirchhoff approaches and one diffraction (Figure 3c).

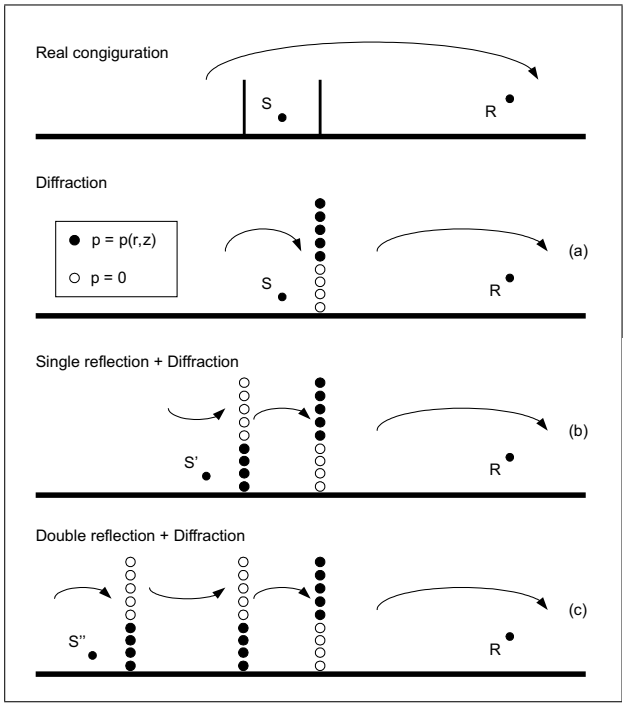

Figure 3. Principle of calculation with two parallel barriers at the order 2 of reflection. In inhomogeneous medium, the curved rays represent the meteorological effects.

3.4. Multiple reflections in inhomogeneous medium

The principle of the GFPE-Kirchhoff method in inhomogeneous medium is presented Figure 3. The presence of two parallel obstacles creates different path of propagation with several reflections. As the direction of propagation changes after each reflection on a barrier, the sound speed profile given equation (12) has to be used alternatively with the sound speed profile from the image-sources to the receiver.

4. Numerical simulations and validations

4.1. Single reflection

4.1.1. Configuration

A realistic road traffic noise configuration with a barrier and an impedance jump is studied. A source is located at a height of 0.5 m in the middle of a 14 m wide road considered as acoustically rigid (air flow resistivity $\sigma_1 = \infty$). A 3 m high barrier stands on the left side of the road. The excess attenuation is calculated at a receiver located at 82 m of the source and a height of 4 m above a grass like ground. The ground impedance is determined by use of the Delany and Bazley formulation [37] with an air flow resistivity $\sigma_2 = 180\,\text{kPa s/m}^2$ and an infinite thickness (Figure 4).

4.1.2. Reflection on a rigid vertical obstacle in homogeneous medium

The barrier used in the configuration described in Figure 4 is considered as acoustically rigid (air flow resistivity

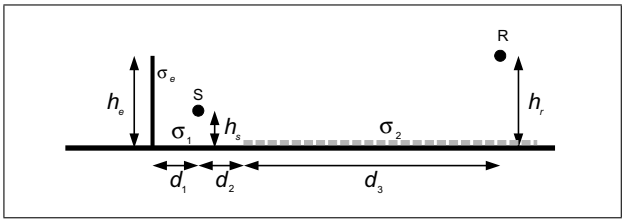

Figure 4. Geometry of the barrier case with an impedance jump. $h_s = 0.5\,\text{m}$, $h_r = 4\,\text{m}$, $h_e = 3\,\text{m}$, $d_1 = 7\,\text{m}$, $d_2 = 7\,\text{m}$, $d_3 = 75\,\text{m}$, $\sigma_1 = \infty$, $\sigma_2 = 180\,\text{kPa s/m}^2$.

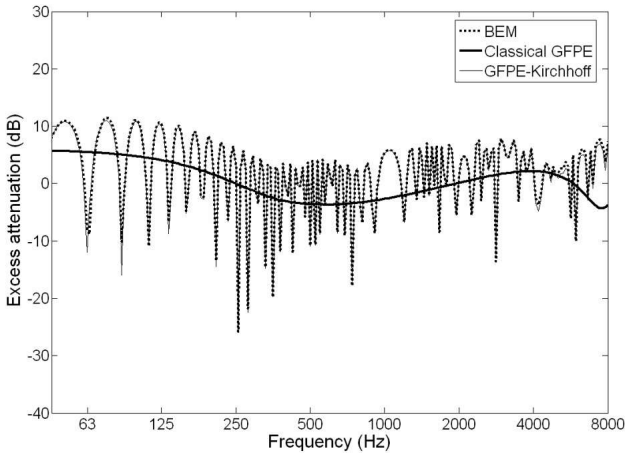

Figure 5. Excess attenuation vs frequency. Comparison between BEM, classical GFPE and GFPE-Kirchhoff calculations results in homogeneous atmosphere for the case described in Figure 4. $\sigma_e = \infty$.

$\sigma_e = \infty$). Classical GFPE and GFPE-Kirchhoff calculations results in homogeneous atmosphere are compared to a reference calculation performed with the BEM (Boundary Element Method [38]). Results are given Figure 5. Differences between classical GFPE and BEM calculations point out the inefficiency of the classical GFPE to study this configuration. On the other hand, the interferences amplitudes and localisations are perfectly respected between BEM and GFPE-Kirchhoff results. Thus, the GFPE-Kirchhoff method is efficient to add simple reflection and backscattering effect in GFPE models.

4.1.3. Reflection on an absorbent vertical obstacle in homogeneous medium

The barrier is now covered by an acoustic absorbent whose air flow resistivity σ_e equals $30\,\text{kPa s/m}^2$. The comparison between GFPE- Kirchhoff with a rigid barrier, BEM with an absorbent barrier and GFPE-Kirchhoff with an absorbent barrier are presented in Figure 6. Excess attenuations calculated with BEM and GFPE-Kirchhoff with absorbent material are very similar for the studied frequency range. This means that the GFPE-Kirchhoff approach is fully appropriate to take material impedances into account in reflections phenomena.

GFPE-Kirchhoff results comparisons between the rigid barrier case and the absorbent barrier one show no significant difference of the excess attenuations at low fre-

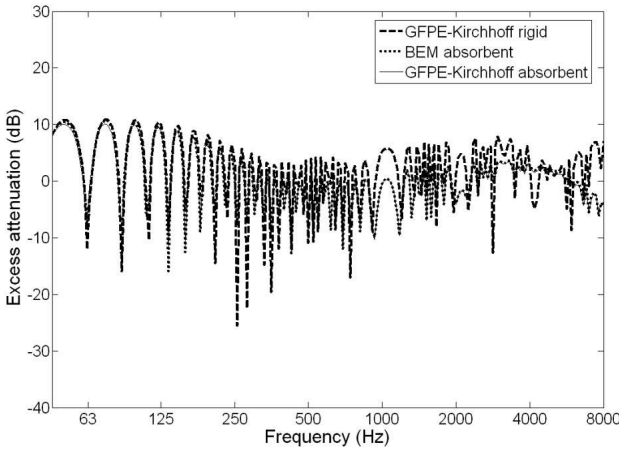

Figure 6. Excess attenuation vs frequency. Comparison between GFPE-Kirchhoff with a rigid barrier, BEM with an absorbent barrier, GFPE-Kirchhoff with an absorbent barrier calculations results in homogeneous atmosphere for the case described in Figure 4. $\sigma_e = 30\,\mathrm{kPa\,s/m^2}$.

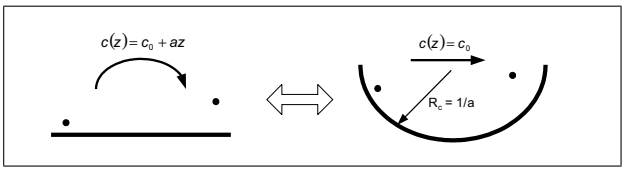

Figure 7. Analogy between sound speed profile and curved surface.

quencies, as expected. On the other hand, the absorbent efficiency increases with frequency and reduces the interferences amplitudes.

4.1.4. Single reflection on a rigid vertical obstacle in inhomogeneous medium

The road traffic noise configuration described in Figure 4 is studied with an inhomogeneous medium. The barrier is considered as acoustically rigid (air flow resistivity $\sigma_e = \infty$). A strong sound speed gradient is chosen to point out the influence of refraction; the sound speed profile corresponding to a downwind propagation condition writes:

$$c(z) = c_0\big(1 + az\big), \tag{13}$$

with the reference sound speed $c_0 = 340\,\mathrm{m/s}$ and the refractive index $a = 4.9 \cdot 10^{-3}/\mathrm{m}$.

Temperature gradient First the sound speed profile given in equation (13) is supposed to be created by vertical temperature variations only. Such a sound speed profile presents the advantage to be possibly introduced in BEM calculation by using the analogy between sound propagation above a flat surface along curved ray paths and sound propagation above a curved surface along straight ray paths [39] (Figure 7).

The methodology discussed in section 3.2 for a temperature gradient is applied to the road traffic configuration described in Figure 4. Figure 8 shows the results obtained

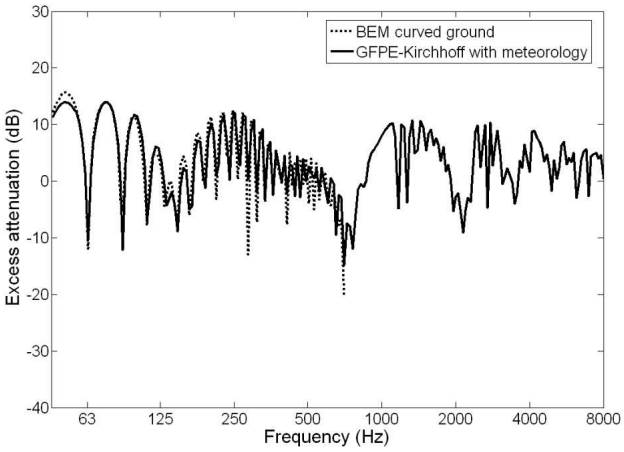

Figure 8. Excess attenuation vs frequency. Comparison between BEM curved ground and GFPE-Kirchhoff calculations results in inhomogeneous atmosphere due to a temperature gradient for the case described in Figure 4. $c(z) = c_0(1 + az)$ with $c_0 = 340\,\mathrm{m/s}$ and $a = 0.0049/\mathrm{m}$.

with GFPE- Kirchhoff approach in the case of inhomogeneous atmosphere compared to BEM in homogeneous atmosphere with an equivalent curved ground (ray of curvature $R_c = 1/a = 1/(4.9 \cdot 10^{-3}) = 5.20\,\mathrm{m}$). The agreement between the two methods is very good. Minimum excess attenuation levels of the GFPE-Kirchhoff results appear at the same frequency as in BEM results and levels are well estimated.

Wind speed gradient The sound speed profile given in equation (13) is now supposed to be created by vertical wind speed variations only. The methodology discussed in section 3.2 for a wind speed gradient is applied to the road traffic configuration described in Figure 4. Thus, a new sound speed profile c', symmetrical about c relatively to the reference sound speed c_0 is used for propagation from image-source S' to the barrier, and writes

$$c'(z) = c_0\big(1 - az\big), \tag{14}$$

GFPE-Kirchhoff results for a sound speed profile due to wind speed variations are compared in Figure 9 to GFPE-Kirchhoff results for a sound speed profile due to a temperature gradient. Up to 500 Hz, the effect of introducing an upward symmetrical sound speed profile c' (instead of c), for the propagation between S' and the barrier, is small. This effect increases with frequency and becomes especially sensible between 700 Hz and 1900 Hz where the excess attenuations difference can reach about 10 dB.

The large value of the refractive index is used to highlight the modelling of meteorological effect in the formulations. A simulation using a more realistic value ($a = 6{\cdot}10^{-3}/\mathrm{m}$) is shown in Figure 10 to give a proper indication of wind gradient effects in real life. GFPE-Kirchhoff results in inhomogeneous conditions are compared to GFPE-Kirchhoff results in homogeneous atmosphere. Amplitudes and locations of interferences between the two results are rather different due to the wind gradient effect.

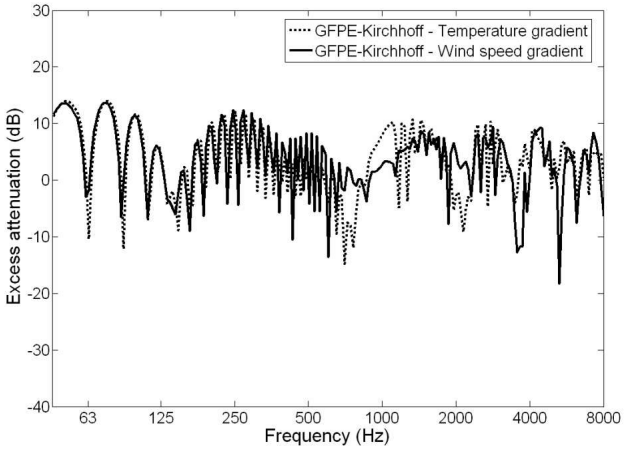

Figure 9. Excess attenuation vs frequency. Comparison between GFPE-Kirchhoff calculations results in inhomogeneous atmosphere due to temperature gradient and GFPE-Kirchhoff calculations results in inhomogeneous atmosphere due to a wind speed gradient for the case described in Figure 4. $c(z) = c_0(1+az)$ with $c_0 = 340$ m/s and $a = 0.0049$/m.

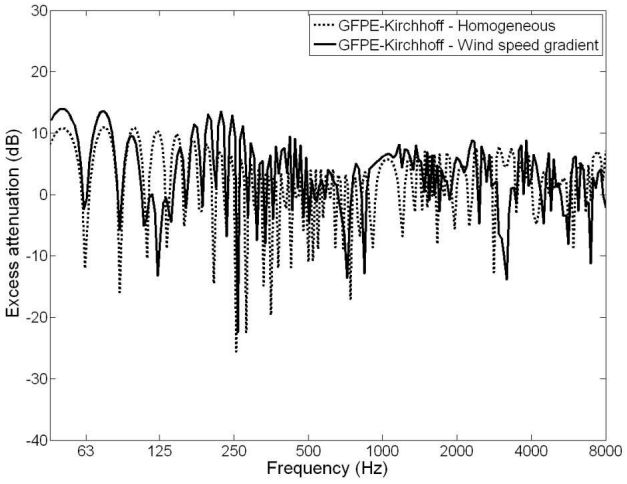

Figure 10. Excess attenuation vs frequency. Comparison between GFPE-Kirchhoff calculations results in homogeneous atmosphere and GFPE-Kirchhoff calculations results in inhomogeneous atmosphere due to a wind speed gradient for the case described in Figure 4. $c(z) = c_0(1 + az)$ with $c_0 = 340$ m/s and $a = 0.006$/m.

This leads to a difference about 2 dB in A-weighted global excess attenuation between homogeneous and inhomogeneous conditions for an emission spectrum of a normalized traffic noise [40].

4.2. Multiple reflections

4.2.1. Configuration

A road configuration with vertical rigid barriers on both sides is studied (Figure 11). A source is located at a height of 0.5 m in the middle of a 14 m wide road considered acoustically rigid (air flow resistivity $\sigma_1 = \infty$). Rigid 3 m high barriers (air flow resistivity $\sigma_e = \infty$) are on each side of the road. The excess attenuation is calculated at a 4 m high receiver located at 82 m of the source above a grass like ground. The ground impedance is determined by use of the Delany and Bazley formulation [37] with an air flow resistivity $\sigma_2 = 180$ kPa s/m^2 and an infinite thickness.

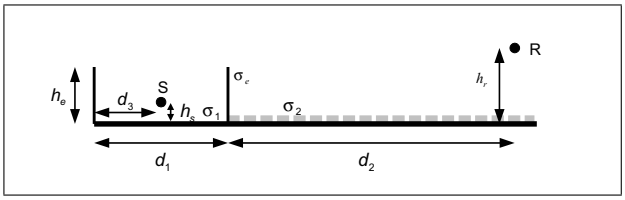

Figure 11. Geometry of road configuration with two barriers. $h_s = 0.5$ m, $h_r = 4$ m, $h_e = 3$ m, $d_1 = 14$ m, $d_2 = 75$ m, $d_3 = 7$ m, $\sigma_1 = \infty$, $\sigma_2 = 180$ kPa s/m^2.

4.2.2. Multiple reflections on rigid vertical obstacles in homogeneous medium

The Configuration described in Figure 11 is studied in homogeneous medium. The GFPE-Kirchhoff approach presented in section 3.3 is used to compute multiple reflections calculations. Comparison between BEM and GFPE-Kirchhoff are presented in Figure 12 for 1st order (one reflection), 6th order (6 reflections), 15th order (15 reflections) and 25th order (25 reflections) of reflections.

Results show the importance of increasing the reflection order when frequency increases. Even if a 6th order of reflection calculation is efficient for frequencies under 800 Hz, the 25th order is required for calculation up to 5000 Hz. Moreover, on a Pentium III 700 MHz, calculation time to get 25th order results is only 25% higher than for 6th order calculations. The 24 Hz frequency interval which separates two interferences is well correlated with distance between the two barriers,

$$c_0/d_1 = 340/14 \approx 24\,\text{Hz}. \tag{15}$$

4.2.3. Multiple reflections on absorbent vertical obstacles in homogeneous medium

The same configuration described below is now studied with two impedant vertical barriers whose air flow resistivity σ_e equals 30 kPa s/m^2. Comparison between BEM and GFPE-Kirchhoff are presented in Figure 13 for 1st order (one reflection), 6th order (6 reflections), 15th order (15 reflections) and 25th order (25 reflections) of reflections.

The energy reflected by the barrier is reduced due to the absorbing layers. Thus less number of reflections is required to achieve a good accuracy between GFPE-Kirchhoff and BEM results. In this case, the solution given by GFPE-Kirchhoff for the 6th order of reflections fits quite well with the BEM for all the frequency range, instead of the case of rigid barriers which need a 25th order of reflection.

4.2.4. Multiple reflections on rigid vertical obstacles in inhomogeneous medium

Multiple reflections principle in inhomogeneous atmosphere presented in section 3.4 is applied to the configuration described in Figure 11. The sound speed profile

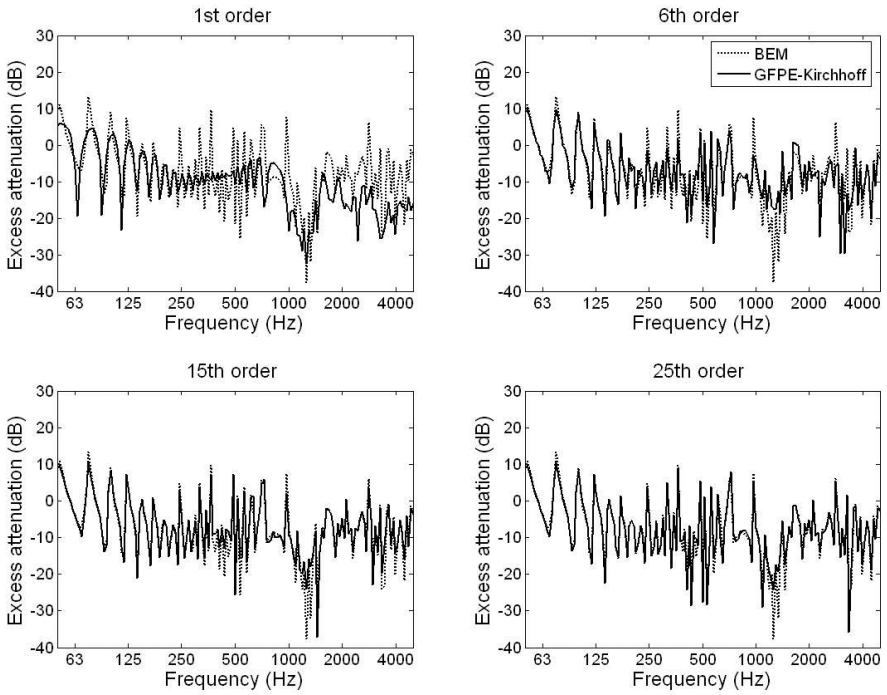

Figure 12. Excess attenuation vs frequency. Comparison between BEM and GFPE-Kirchhoff calculations results in homogeneous atmosphere with two rigid barrier ($\sigma_e = \infty$) for the case described in Figure 11 for the 1st order, 6th order, 15th order and 25th order of reflection.

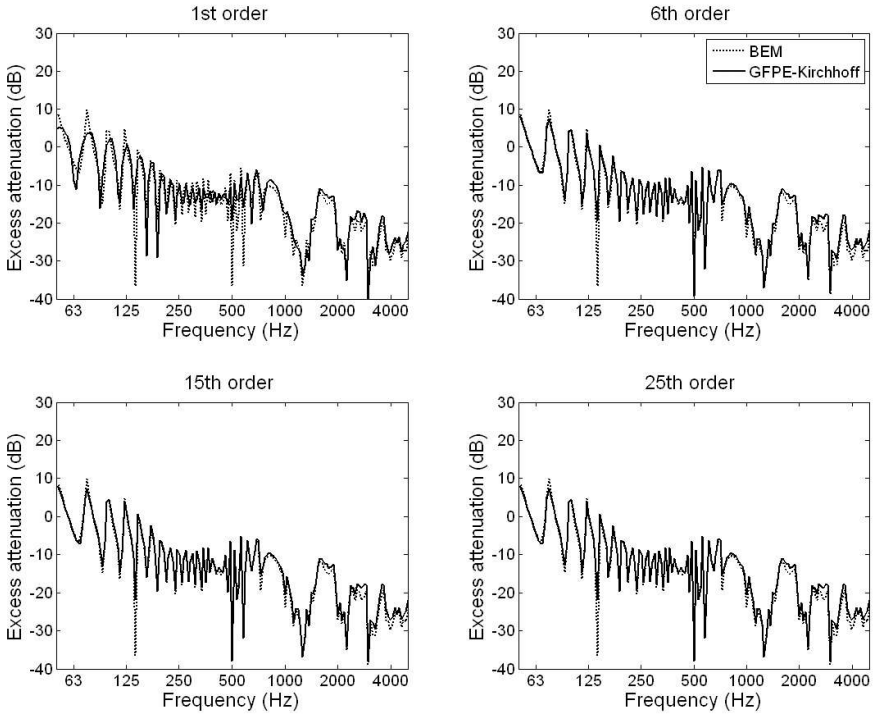

Figure 13. Excess attenuation vs frequency. Comparison between BEM and GFPE-Kirchhoff calculations results in homogeneous atmosphere with two absorbent barriers ($\sigma_3 = 30\,\mathrm{kPa\,s/m^2}$) for the case described in Figure 11 for the 1st order, 6th order, 15th order and 25th order of reflection.

given by equation (13) is used. It is supposed to be created by vertical wind speed variation only. Because of the presence of the two barriers, multiple propagation path lead to use a new sound speed profile c', symmetrical about c relatively to reference sound speed c_0 (equation 14). Thus, for each reflection on one of the two barriers, the image source method requires to apply c and c' alternatively.

Calculations are performed up to the 25th order of reflections. Results given by GFPE-Kirchhoff calculations in inhomogeneous medium are compared with GFPE-Kirchhoff in homogeneous atmosphere (Figure 14). The results point out the importance of the meteorological effects. For a typical traffic noise spectrum at emission [41], the difference in A-weighted sound levels calculated in ho-

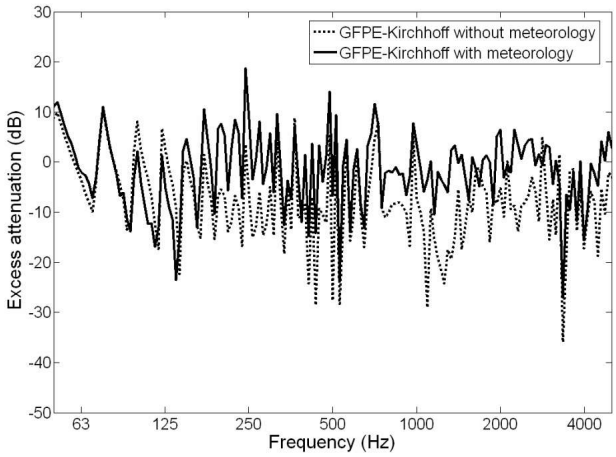

Figure 14. Excess attenuation vs frequency. Comparison between GFPE-Kirchhoff calculations results in homogeneous atmosphere and GFPE-Kirchhoff calculations results in inhomogeneous atmosphere for the case described in Figure 11.

mogeneous and downward conditions is about 6 dB. Even if a strong sound speed profile has been chosen to point out the meteorological effect, it is interesting to note the decrease of the barrier efficiency in downward conditions.

5. Conclusion

The principle of the GFPE-Kirchhoff method and its applications to realistic traffic noise configurations has been presented. The results for three different studied configurations show that the complementary Kirchhoff approach is efficient for backscattering integration in the GFPE method. More precisely, the comparison of numerical results with BEM calculations shows that the method is well adapted to solve multiple reflections problems on vertical obstacles and allows to deal with impedant or rigid surfaces both in homogenous or inhomogeneous media. This approach could be easily extended to other PE models such as the SPPE [42] (Split-step Padé Parabolic Equation) and the SFPE [43] (Split-step Fourier Parabolic Equation). Works are in progress in order to investigate more complex range dependant wind speed profiles.

References

[1] J. Defrance, Y. Gabillet: A new analytical method for the calculation of outdoor noise propagation. Applied Acoustics **57** (1999) 109–127.

[2] M. C. Berengier, B. Gauvreau, P. Blanc-Benon, D. Juve: Outdoor sound propagation: A short review on analytical and numerical approaches. Acta Acustica united with Acustica **89** (2003) 980–991.

[3] D. Heimann, G. Gross: Coupled simulation of meteorological parameters and sound level in a narrow valley. Applied Acoustics **56** (1999) 73–100.

[4] M. West, Y. Lam: Prediction of sound fields in the presence of terrain features which produce a range dependant meteorology using the generalised terrain parabolic equation (GT-PE) model. Internoise, Nice, France, 2000.

[5] D. K. Wilson, J. Noble: Putting meteorology into outdoor sound propagation calculations. Internoise, Nice, France, 2000.

[6] S. J. Franke, G. W. Swenson: A brief tutorial on the fast field program (FFP) as applied to sound propagation in the air. Applied Acoustics **27** (1989) 203–215.

[7] Y. L. Li, M. J. White, S. J. Franke: New fast field programs for anisotropic sound propagation through an atmosphere with a wind velocity profile. J. Acoust. Soc. Am. **95** (1994) 718–726.

[8] R. Raspet, S. W. Lee, E. Kuester, D. C. Chang, W. F. Richards, R. Gilbert, N. Bong: A fast-field program for sound propagation in a layered atmosphere above an impedance ground. J. Acoust. Soc. Am. **77** (1985) 345–352.

[9] C. F. Chien, W. W. Soroka: Sound propagation along an impedance plane. Journal of Sound and Vibration **43** (1975) 9–20.

[10] A. L'Esperance, P. Herzog, G. A. Daigle, J. Nicolas: Heuristic model for outdoor sound propagation based on an extension of the geometrical ray theory in the case of a linear sound speed profile. Applied Acoustics **37** (1992) 111–139.

[11] F. B. Jensen, W. A. Kuperman, M. B. Porter, H. Schmidt: Computational ocean acoustics. AIP Press ed. 2000, Springer-Verlag, New-York, 2000.

[12] E. M. Salomons: Computational atmospheric acoustics. Kluwer Academic, 2001.

[13] V. Cerveny, M. M. Popov, I. Psencik: Computation of wave fields in homogeneous media. Gaussian beam approach. Geophys. J. R. Astr. Soc. **70** (1982) 109–128.

[14] M. B. Porter, H. P. Bucker: Gaussian beam tracing for computing ocean acoustic fields. J. Acoust. Soc. Am. **82** (1987) 1349–1359.

[15] Y. Gabillet, H. Schroeder, G. A. Daigle, A. L'Esperance: Application of the Gaussian beam approach to sound propagation in the atmosphere: Theory and experiments. J. Acoust. Soc. Am. **93** (1993) 3105–3116.

[16] R. Blumrich, D. Heimann: A linearized Eulerian sound propagation model for studies of complex meteorological effects. J. Acoust. Soc. Am. **112** (2002) 446–455.

[17] F. D. Tappert: The parabolic approximation method. – In: Wave propagation and underwater acoustics. J. B. Keller, J. S. Papadakis (eds.). Springer, New York, 1977, 224–287.

[18] K. E. Gilbert, M. J. White: Application of the parabolic equation to sound propagation in refracting atmosphere. J. Acoust. Soc. Am. **85** (1989) 630–637.

[19] M. West, K. E. Gilbert, R. A. Sack: A tutorial on the parabolic equation (PE) model used for long range sound propagation in the atmosphere. Applied Acoustics **37** (1992) 31–49.

[20] K. Attenborough, S. Taherzadeh, H. E. Bass, R. Raspet, G. R. Becker, A. Gudesen, A. Chrestman, G. A. Daigle, A. L'Esperance, Y. Gabillet, Y. Gabillet, Y. L. Li, M. J. White, P. Naz, J. M. Noble, H. A. J. M. van Hoof: Benchmark cases for outdoor sound propagation models. J. Acoust. Soc. Am. **97** (1995) 173–191.

[21] M. Galindo, M. R. Stinson, G. A. Daigle: Comparaison of some methods used for prediction of atmospheric sound propagation. Canadian Acoustics **25** (1997) 3–11.

[22] H. M. McDonald: Diffraction at a straignt edge. Proceed. London Math. Soc. **2** (1915) 103–105.

[23] A. D. Pierce: Diffraction of sound around corners and over wide barriers. J. Acoust. Soc. Am. **55** (1974) 941–955.

[24] M. Buret, K. M. Li: Diffraction of sound from a dipole source near to a barrier or an impedance discontinuity. J. Acoust. Soc. Am. **113** (2003) 2480–2494.

[25] P. J. T. Filippi: Theoretical and numerical study of diffraction by a thin screen (in French). Acustica **21** (1969) 343–350.

[26] B. A. De Jong, E. Stusnick: Scale model studies of the effects of wind on acoustics barrier performance. Noise Control Eng. J. **6** (1976) 101–109.

[27] E. M. Salomons: Rediction of the performance of a noise screen due to screen-induced wind-speed gradients. Numerical computations and wind-tunnel experiments. J. Acoust. Soc. Am. **105** (1999) 2287–2293.

[28] M. D. Collins, R. B. Evans: A two-way parabolic equation for acoustic backscattering in the ocean. J. Acoust. Soc. Am. **91** (1992) 1357–1368.

[29] M. West, Y. Lam: A two-way vertical interface parabolic equation (tv-pe) model for atmospheric propagation in the presence of severe terrain features. 9th International Symposium on Long Range Sound Propagation, Amsterdam, Netherlands, 2000.

[30] K. E. Gilbert, X. Di: A fast Green's function method for one-way sound propagation in the atmosphere. J. Acoust. Soc. Am. **94** (1993) 2343–2352.

[31] X. Di, K. E. Gilbert: Application of a fast Green's function method to long range sound propagation in the atmosphere. 5th International Sympsium on Long Range Sound Propagation, 1992.

[32] E. M. Salomons: Improve Green's function parabolic equation method for atmospheric sound propagation. J. Acoust. Soc. Am. **104** (1998) 100–111.

[33] N. Barriere, Y. Gabillet: Sound propagation over a barrier with realistic wind gradients. Comparaison on wind tunnel experiment with GFPE computation. Acustica united with Acta Acustica **85** (1999) 325–334.

[34] F.-E. Aballea: Outdoor sound propagation: Application of the fast parabolic equation to meteorological effects and complex topographies (in French). Thesis, Université du Maine, Le Mans, France, 2004.

[35] F. Aballea, J. Defrance: Simple and multi-reflections using the PE method with a complementary Kirchhoff approximation. 7ème Congrès Français d'Acoustique, Strasbourg, France, 2004.

[36] E. M. Salomons: Diffraction by a screen in downwind sound propagation: A parabolic-equation approach. J. Acoust. Soc. Am. **95** (1994) 3109–3117.

[37] M. E. Delany, E. N. Bazley: Acoustical properties of fibrous absorbent materials. Applied Acoustics **3** (1970) 105–116.

[38] P. Jean: A variational approach for the study of outdoor sound propagation and application to railway noise. Journal of Sound and Vibration **212** (1998) 275–294.

[39] K. M. Li, Q. Wang: A BEM approach to assess the acoustic performance of noise barriers in a refracting atmosphere. Journal of Sound and Vibration **211** (1998) 663–681.

[40] EN 1793-3:1997, Road traffic noise reducing devices - Test method for determining the acoustic performance - Part 3: Normalized traffic noise spectrum.

[41] EN 1793-3:1997, Road traffic noise reducing devices - Test method for determining the acoustic performance - Part 3. Normalized traffic noise spectrum.

[42] M. D. Collins: A split-step Padé approximation solution for the parabolic equation method. J. Acoust. Soc. Am. **93** (1993) 1736–1742.

[43] D. J. Thomson, N. R. Chapman: A wide-angle split-step algorithm for the parabolic equations. J. Acoust. Soc. Am. **74** (1983) 1848–1854.